

자기정렬에 의한 평판전극 마이크로미러 어레이의 설계와 제작

유병욱<sup>1</sup>, 김민수<sup>1</sup>, 진주영<sup>1</sup>, 전진아<sup>2</sup>, 박재형<sup>2</sup>, 김용권<sup>1</sup>

<sup>1</sup>서울대학교 전기컴퓨터공학부

<sup>2</sup>이화여자대학교 물리학과

Design and Fabrication of Self-aligned Parallel-plate Type Micromirror Array

Byung-Wook Yoo, Minsoo Kim, Joo-Young Jin, Jin-A Jeon, Jae-Hyong Park, and Yong-Kweon Kim

<sup>1</sup>School of Electrical Engineering and Computer Science, Seoul National University

<sup>2</sup>Department of Physics, Ewha Womans University

**Abstract** - We present an one-axis parallel-plate type of bulk micromachined torsional micromirror array with single crystalline silicon (SCS) fabricated on the glass substrate. Structurally, bottom electrodes (amorphous silicon) in this mirror are DRIEd along the aluminum mirror patterns on SCS, which are self-aligned with mirror plates. Tracing the history of the micromirror study, we found that few papers have been published on research for uniform driving voltages based upon the tilting direction. If there is a slight misalignment during anodic bonding between top (mirror plate) and bottom electrodes, the non-uniformity of driving voltage will be led depending on two different tilting direction. This paper discusses how much the pull-in voltages can be different due to misalignment between two electrodes. Moreover, We achieve uniform pull-in voltage regardless of misalignments in photolithography and anodic-bonding between two individual layers.

1. Introduction

Micromirrors have been studied as the most important devices in the field of optical micro electromechanical systems (MEMS). There are various mechanisms to actuate the micromirror devices and different actuation mechanisms let the designed micromirrors perform the desired motions properly. Among them, such as mechanical, piezoelectric, thermal and others, electrostatic torsional actuation mechanism is the most popular due to its easier static control, better dynamic response, less parasitic effects such as buckling.

Although mentioned above about its better performances, challenges or problems for specific things of torsional micromirrors still exist. Here in this paper, experimental validation of static behavior (pull-in) uniformity has been carried out on a fabricated micromirror and compared to the simulation results in terms of the misalignment between top (mirror plate) and bottom electrodes.

2. Modeling of the torsional micromirror

The schematic views of the torsional micromirror is shown in Figure 1. Dimensions of the designed micromirror are 320 by 320 μm<sup>2</sup> in length and 7.1 μm in thickness. Moreover, dimensions of their spring are 30 μm in length, 2 μm in width and the same as a mirror plate in thickness. Material of the micromirror is SCS deposited by an aluminum lift-off.

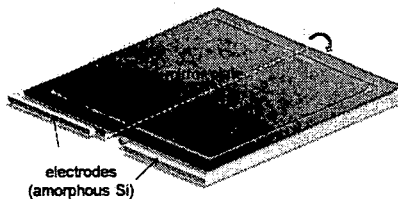


Figure 2. Schematic view of the SCS torsional micromirror

Two torsional springs are attached to the center of the micromirror. The micromirror is thus suspended and designed to be refrained from lateral motion based on Eq. (1).

$$\frac{k_t}{k_b} = \frac{1}{16(1 + \nu)} \left( \frac{w_s l_s}{t_s} \right)^2 \quad (1)$$

$k_t$  and  $k_b$  are torsional stiffness and bending stiffness respectively.  $w_s$ ,  $l_s$ , and  $t_s$  are the width, length, and thickness of

the spring, respectively.  $\nu$  is silicon Poisson's ratio. The relative ratio between torsional and bending motions is derived as Eq. (1). The smaller the relative ratio is, the better the performance of springs is during torsional motion. Therefore, spring width is designed to be thin as 2 μm. Although spring width could be set as thin as possible, the length and thickness of the spring cannot be simply determined due to trade-off relationship with low driving voltage.

The finite radius of curvature (ROC) is set by the bimetallic deformation on SCS mirror plate by Eq. (2) [1].

$$R = \frac{E_s d_s^2}{6\sigma_f (1 - \nu_s) d_f} \quad (2)$$

$d_s$ ,  $d_f$ ,  $E_s$  and  $\nu_s$  are silicon thickness, film thickness, silicon Young's modulus and film stress, respectively. ROC is proportional to the square of the silicon thickness and inversely metal film layer thickness. Hence, it is necessary to make a mirror-frame thickness thick or compensate stress by deposition metal on both sides of the mirror. Although aluminum deposition is designed to be used for one side as a reflective material, the opposite side of a mirror-frame cannot be easily deposited by aluminum due to SOI wafer bulk machining and bonding process. Reflective material, aluminum, is properly set to be 100 nm so as to hold its reflectivity as well as ROC fit to its application, space telescope.

Resonance frequency is determined around 10 kHz, first of all, for the stability. With a constant device thickness, correlation among dimensions of the torsional micromirror is considered as Figure 2 through MATLAB calculations. All the dimensions of the micromirror are achieved also in consideration of low driving voltage and high ROC.

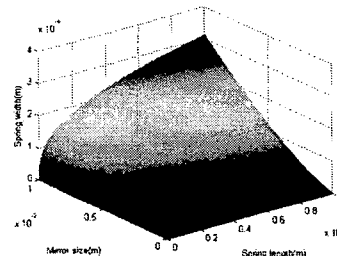


Figure 2. Relationship among various dimension of a micromirror and springs

Array size is designed up to 10 by 10 and fill factor is 85 %. Simulated pull-in voltage is 35.11 V. Though full torsional angular deflection is 2.76 degree in terms of the gap, 7.7 μm, between electrodes, bottom electrode area is designed to be desirably controlled up to 1.29 degree.

As for bottom electrode design, amorphous silicon on glass substrate is shaped at the final process of DRIE. Just after DRIE defines the mirror plates, springs and the whole shape of the array, DRIE consequently divides the amorphous silicon on glass into electrodes and ground shield.

### 3. Fabrication

#### 3.1 Micromachining process

The SCS based parallel-plate electrostatic micromirror combining with SOI structure gain in simpler process design with anodic alignment bonding. Figure 3 depicts the three dimensional and cross-section drawings of fabrication process.

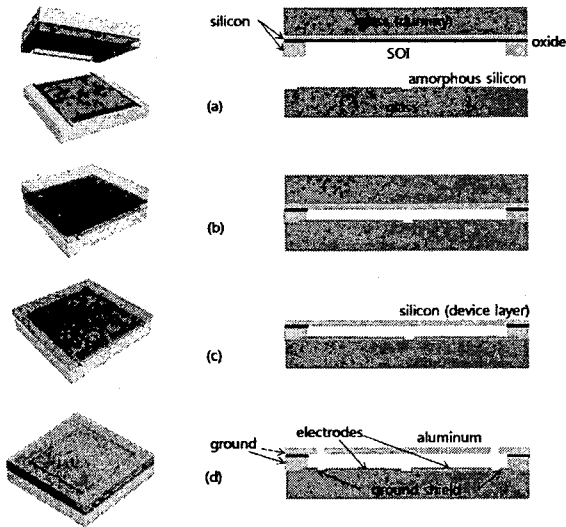


Figure 3. Fabrication process flow

To begin with, dummy glass wafer is anodic-bonded to device layer of the SOI wafer in order to handle the SOI structure. After handling layer of the SOI wafer is thinned and polished up to the gap between the mirror plate and bottom electrode, the gap is set in the initial step of DRIE process on the whole. Amorphous silicon on glass substrate is patterned by DRIE process to separate two bottom electrodes (Figure 3(a)). Exposed buried oxide of the SOI wafer is removed so that gap is finally defined. Another anodic bonding of the bonded SOI wafer with patterned glass wafer is performed. Bonding condition is 800 V, 600 N, and 380 degrees (Figure 3(b)). After Cr/Au deposition and PR passivation of the backside of glass wafer patterned with electrodes, HF wet etching gets rid of the dummy glass wafer which helps handling of a device layer (Figure 3(c)). Then, aluminum is deposited by thermal evaporation and lifted-off for not only a DRIE mask material, but also a reflective metal surface. DRIE releases the micromirror structure (top electrode) substantially as well as the bottom electrode and ground shield simultaneously. Ground shield is pressed down from one of the silicon layer directly by means of anodic bonding and separated by DRIE from the bottom electrode (Figure 3(d)). Since DRIE defines along the aluminum patterns on the device layer, bottom electrode gets self-aligned and defined exactly the same as the micromirror shape. Driving voltages to each tilting direction, therefore, can be fairly similar each other. The remnants of amorphous silicon (ground shield) is grounded under the handling layer of SOI wafer by anodic-bonding. ground shield keeps charges from injection and trapping into the glass substrate as well. Simply put, charging effect is designed to be properly prevented from peripheral dielectric charging [2].

#### 3.2 Fabricated micromirror

Micromirror fabrication in this work is based on the consideration of large reflective area and soft torsional springs. Amorphous silicon is deposited on the glass substrate forming the bottom electrodes that has the same dimension as that of the micromirror. Aluminum layer is deposited on the mirror plate covering all the surface of the micromirror and segments of two torsional springs, forming the top electrode which is grounded. At the ends of the mirror plate, there are two landing tips in order to prevent stiction. Figure 4 illustrates the SEM photos of fabricated micromirror. The mirror plate is 320  $\mu\text{m}$  each side. From the enlarged view of a torsional spring, scallops from DRIE is clearly shown. TDMR-AR87 is used as a photoresist to fabricate 30  $\mu\text{m}$ -length and 2  $\mu\text{m}$ -width spring.

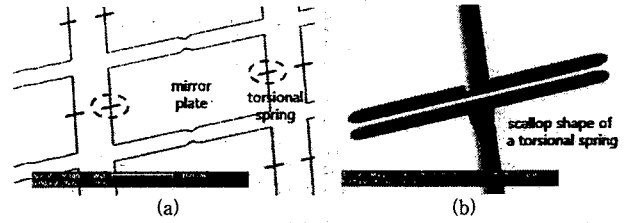


Figure 4. Fabrication results (a) SEM photo of the micromirror device. (b) SEM photo of scallop shape of a torsional spring generated by DRIE process.

### 4. Discussion

A relatively small mechanical tilting angle, 2.76 degree, was achieved due to the thinning process fault during the fabrication. A preferably same working range away from the unstable pull-in status towards each tilting direction could be achieved thanks to two self-aligned bottom electrodes having the same dimension under the mirror plate. This conforms to uniform pull-in voltage towards any tilting direction. According to Figure 5, if there is a misalignment during anodic bonding and photolithography process, driving and pull-in voltages towards each tilting angle result in different values. When no misalignment, a micromirror touches down at 35.11 V from analytical calculation. Although a large mirror, such as this one (320 by 320  $\mu\text{m}^2$ ), is insensitive to a electrode misalignment due to low driving voltage, 5  $\mu\text{m}$  misalignment still leads the pull-in voltage to be increased by 1.85 V, up to 36.96 V. We measured four micromirrors among 2 by 2 array. Although 5  $\mu\text{m}$  misalignment was measured during bonding, only 0.85 V (average) differed between pull-in voltages towards individual tilting directions. Standard deviation was 1.18.

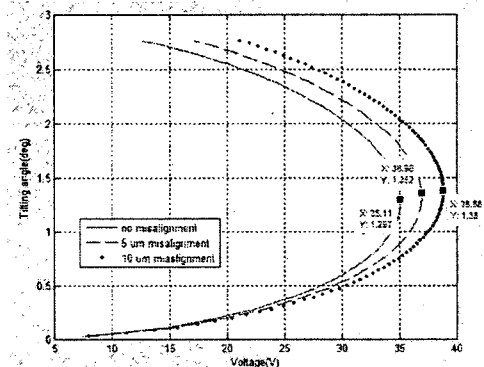


Figure 5. Simulation result of pull-in spots based on the extent of the misalignment.

Pull-in voltage was measured as 28.59 V on the average, which is less than the calculated value (35.11 V) in Figure 5 due to the thinned spring width by 0.2  $\mu\text{m}$  from DRIE.

### 5. Conclusion

This paper describes the design, fabrication, and test result of an one-axis parallel-plate type of the torsional micromirror array with SCS. Self-aligned electrode design using DRIE process has been introduced that allows fairly similar pull-in voltages among micromirrors regardless of the extent of misalignment. Similar pull-in voltages, furthermore, conforms to uniform driving voltages over orientations of individual mirrors. When a micromirror array allows delicate control over orientations of individual mirrors, this could weigh with a variety of image forming application.

### References

- [1] Mehmet R. Dokmeci, et al., "Two-axis single-crystal silicon micromirror arrays", *J. Microelectromechanical Syst.*, vol. 13, no. 6, pp. 1006-1017, 2004.
- [2] K. W. Goosen, et al., "Charging effects in electrostatically-actuated membrane devices", *the SPIE Conf. on Miniaturized Systems with Micro-Optics and MEMS 1999*, Santa Clara, CA, vol. 3878, pp. 407-415.